The Astrophysical Journal Letters, 768:L3 (5pp), 2013 May 1 doi:10.1088/2041-8205/768/1/L3

POLARIZED EXTENDED Lyα EMISSION FROM A $z = 2.3$ RADIO GALAXY

A. Humphrey[1], J. Vernet[2], M. Villar-Martín[3], S. di Serego Alighieri[4], R. A. E. Fosbury[2], and A. Cimatti[5]
[1] Centro de Astrofísica da Universidade do Porto, Rua das Estrelas, 4150-762 Porto, Portugal; andrew.humphrey@astro.up.pt
[2] European Southern Observatory, Karl-Schwarzschild-Strasse 2, D-85748 Garching, Germany
[3] Centro de Astrobiología (INTA-CSIC), Carretera de Ajalvir, km 4, E-28850 Torrejón de Ardoz, Madrid, Spain
[4] INAF-Osservatorio Astrofisico di Arcetri, L.go E. Fermi 5, I-50125 Firenze, Italy
[5] Dipartimento di Astronomia, Università di Bologna, Via Ranzani 1, I-40127 Bologna, Italy
Received 2013 January 14; accepted 2013 February 11; published 2013 April 11

ABSTRACT

We present spatially resolved spectropolarimetric measurements of the 100 kpc scale gaseous environment of the $z = 2.34$ radio galaxy TXS 0211−122. The polarization level of the narrow Lyα emission is low centrally ($P < 5\%$), but rises to $P = 16.4\% \pm 4.6\%$ in the eastern part of the nebula, indicating that the nebula is at least partly powered by the scattering of Lyα photons by H I. Not only is this the first detection of polarized Lyα around a radio-loud active galaxy, it is also the second detection to date for any kind of Lyα nebula. We also detect a pair of diametrically opposed UV continuum sources along the slit, at the outer edges of the Lyα nebula, which we suggest may be the limb of a dusty shell, related to the large-scale H I absorbers often associated with high-z radio galaxies.

Key words: galaxies: active – galaxies: high-redshift – galaxies: individual (TXS 0211–122) – ISM: jets and outflows

Online-only material: color figure

1. INTRODUCTION

Luminous high-redshift Lyα nebulae promise to yield significant insights into the physics of massive galaxy formation (e.g., Mori & Umemura 2006). As prodigious sources of H I Lyα λ1216 photons, they provide an efficient way to select distant galaxies expected to be undergoing phases of significant mass assembly (e.g., Steidel et al. 2000).

What powers the Lyα emission from these nebulae? This question is fundamental to our understanding of the nature and evolutionary status of these enigmatic objects and their central galaxies. A number of ideas have been discussed in the literature, the most promising of which are: (1) cooling radiation emitted during the infall of gas into the dark matter halos of massive protogalaxies (e.g., Haiman et al. 2000); (2) mechanical energy injected by supernovae during powerful starbursts (e.g., Taniguchi & Shioya 2000); (3) scattering of Lyα photons by neutral hydrogen halos around massive, Lyα-emitting galaxies (e.g., Villar-Martín et al. 1996; Zheng et al. 2011); or (4) photoionization by luminous active galactic nuclei (AGNs) and/or young stars (e.g., Villar-Martín et al. 2003; Prescott et al. 2012). While there is currently no consensus concerning which powering mechanism is dominant, it is now clear that no single mechanism is able to explain all Lyα nebulae (e.g., Smith & Jarvis 2007; Prescott et al. 2009, 2012).

Scattering of Lyα photons by neutral hydrogen can result in a net observed polarization in the Lyα emission. Polarimetry is thus a promising way to distinguish between scattering and in situ production of the Lyα photons (e.g., Dijkstra & Loeb 2008). Due to the challenges and observational expense involved, polarization measurements of spatially extended Lyα emission until now had been attempted for only two Lyα nebulae. Prescott et al. (2011) presented imaging polarimetry of the Lyα emission from a giant Lyα nebula associated with a radio-quiet active galaxy at $z = 2.66$, but did not detect significant polarization. Hayes et al. (2011) targeted a large Lyα nebula in a protocluster region at $z = 3.09$, again using narrowband imaging polarimetry, and detected polarized Lyα. They measured $P = 11.9\% \pm 2\%$ within a radius of 7″, with a trend for P to be higher at larger radii, or in regions of low Lyα surface brightness, and with electric field vectors consistent with illumination by a central source. A clear general picture of the polarization properties of high-redshift Lyα nebulae has not yet emerged, and more nebulae, with a wider range of properties, now need to be tested.

The resonant nature of Lyα also allows the detection of associated gaseous structures in front of the Lyα-emitting source. Many giant Lyα nebulae do indeed show strong H I absorption features in their Lyα velocity profile (e.g., van Ojik et al. 1997; Fosbury et al. 2003; Wilman et al. 2005; Humphrey et al. 2008a). These H I absorption features are usually detected across the full spatial extent of the Lyα emission, and usually show a blueshift from the center of the Lyα emission (see van Ojik et al. 1997), implying that the absorber is an expanding shell surrounding the Lyα nebula (Binette et al. 2000). The minimum shell radius, typically about $\gtrsim$50 kpc, allows important constraints on other properties of the shells (mass, kinetic energy, etc.; e.g., van Ojik et al. 1997; Binette et al. 2006; Humphrey et al. 2013). Detecting these absorbing structures in *emission* would substantially improve our understanding of their physical properties, their spatial location, and their origins.

In this Letter, we analyze deep spectroscopy and spectropolarimetry of TXS 0211−122, a $z = 2.34$ radio galaxy known to be associated with a 100 kpc scale Lyα nebula, and with a $\geqslant$100 kpc scale H I absorbing structure (van Ojik et al. 1994, 1997). We aim to probe the geometry, powering mechanism, and origin of the nebular and absorbing structures in this galaxy's gaseous environment. Understanding the physics of these systems is also important to shed light on the relevant feedback processes in the formation and evolution of massive galaxies. We assume $H_0 = 71$ km s^{-1} Mpc^{-1}, $\Omega_\Lambda = 0.73$, and $\Omega_m = 0.27$, with 1″ corresponding to 8.30 kpc at $z = 2.34$.

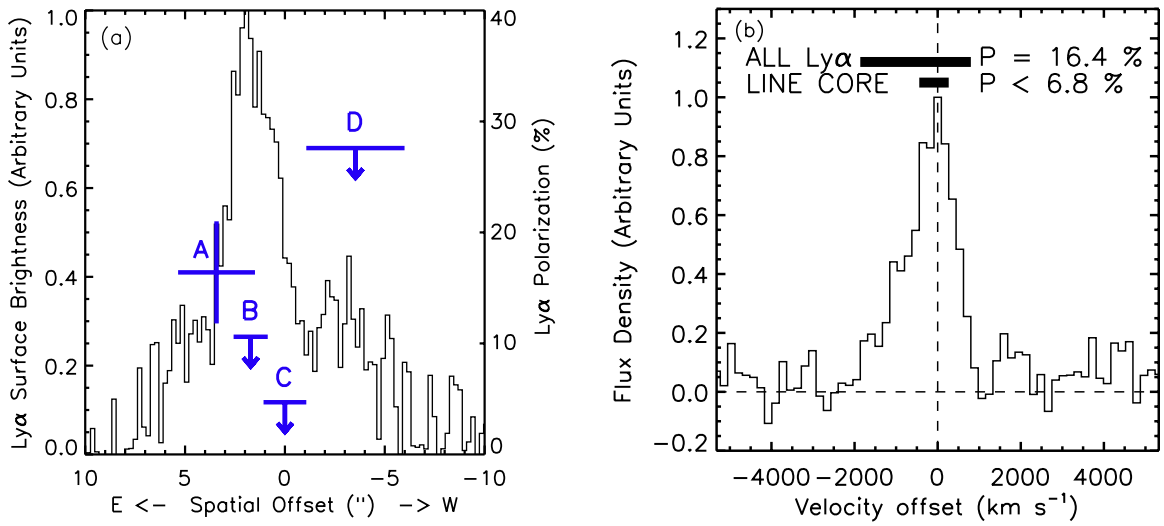

Figure 1. (a) Spatial profile of continuum-subtracted Lyα emission along the slit (continuous curve; left axis), with the Lyα polarization measurements (points A–D; right axis; aperture definition given in Table 1). The spatial zero is the peak of the UV continuum. (b) The spectral region around Lyα in Aperture A, with Lyα polarization measurements in two spectral apertures.

(A color version of this figure is available in the online journal.)

2. OBSERVATIONS

TXS 0211−122 was observed using the Low Resolution Imaging Spectrometer (Oke et al. 1995) in polarimetry mode (Goodrich et al. 1995), in subarcsecond seeing at the Keck II telescope, during 1997 December 24–26. The 300 line mm^{-1} grating and 1″ wide slit resulted in an instrumental profile (IP) of 10 Å, a dispersion of 2.4 Å pixel^{-1}, and a spectral range of ∼3900–9000 Å (∼1200–2700 Å in the rest frame). The 24″ long slit was oriented approximately along the major axis of the radio source (P.A. = 104°, north through east), to maximize signal to noise (S/N) for extended emission. The total on-object exposure time was 28,580 s, split into four sets of integrations, each with four integrations with the half-wave plate successively at P.A. = 0°, 45°, 22.°5, 67.°5. Full details are given by Vernet et al. (2001, V01 hereinafter).

The target was also observed using ISAAC (Moorwood et al. 1998) in long-slit mode at the Very Large Telescope, on 1999 November 27–28. The lines [O II] λ3727, [O III] λλ4959, 5007, and Hα lie in relatively transparent regions of the *J*, *H*, and *K* bands, and integration times were 5200 s, 7200 s, and 7200 s, respectively. The low-resolution grating was used with a 1″ slit to give an IP of ∼30 Å in *J* and *H* bands, and ∼50 Å in the *K* band. The slit P.A. was also 104°. Complete details of the ISAAC data are given by Humphrey et al. (2008b).

3. A POLARIZED Lyα NEBULA

As previously discussed by van Ojik et al. (1994) and Villar-Martín et al. (2003), TXS 0211−122 is associated with an extended Lyα, C IV λ1549 and He II λ1640 nebula, which shows a total Lyα extent along the slit of ∼13″, or ∼110 kpc. Its He II velocity curve displays kinematics that overall are very quiescent (Villar-Martín et al. 2003), consistent with infall (Humphrey et al. 2007), although near the galactic nucleus an excess of emission in the blue wing of He II suggests the presence of outflowing gas in addition (Humphrey et al. 2006). At least in the bright, central few tens of kpc, the nebula is ionized predominantly by the radiation field of the AGN, and has approximately solar metallicity (V01; Humphrey et al. 2008b). The spatial distribution of the Lyα emission along the slit is strikingly asymmetrical compared to the continuum and the other emission lines (Figures 1 and 2), suggesting that the Lyα emission is either strongly absorbed, or is powered by a different mechanism than the other lines (see also van Ojik et al. 1994; Villar-Martín et al. 2003; Humphrey et al. 2007).

The polarization of the Lyα emission line can provide useful constraints on which excitation process powers the giant Lyα nebula (e.g., Dijkstra & Loeb 2008; Dijkstra & Kramer 2012). To this end, we have taken polarization measurements of the Lyα emission at different spatial positions along the slit. Wavelength intervals were defined as the contiguous range of dispersion pixels with Lyα detected at S/N $\geqslant$ 2 pixel^{-1}. Sky-subtraction was performed using a line- and continuum-free spatial bin covering an identical spectral range. Unbiased values of the percentage polarization were estimated according to Simmons & Stewart (1985), and uncertainties were determined using a Monte Carlo method considering detector noise and background polarization (Vernet 2000). Throughout this analysis we adopt the spatial peak of the UV continuum (and Hα emission) along the slit as our fiducial position of the galactic nucleus of the radio galaxy. Table 1 and Figure 1 give the results of our Lyα polarization measurements. All upper or lower limits quoted in this Letter are 3σ.

We detect polarized Lyα emission, with $P = 16.4\% \pm 4.6\%$ (S/N = 3.6) and a P.A. of 154° ± 8°, in a region 1.″50–5.″35 east of the nucleus (Aperture A in Table 1 and Figure 1). The wavelength range covered by this aperture (4046–4081 Å) was chosen to cover the full extent in wavelength space of the Lyα emission, which has an integrated S/N of 32. Weak continuum emission is also present at this position, with $P = 15.3\% \pm 3.3\%$ and P.A. = 194° ± 6° measured in a wide bin covering the relatively line-free continuum region between the wavelengths of the N V and C IV lines. Thus, we have repeated the Lyα polarization measurement after subtracting the continuum emission that lies immediately redward of Lyα (and N V) at 4090–4140 Å, resulting in the noisier but nonetheless consistent measurement $P = 23.1\% \pm 7.1\%$ with P.A. = 143° ± 8°. The core of Lyα emission (4067–4074 Å), however, does not show significant polarization at this spatial position ($P \leqslant 6.8\%$). In the same spatial aperture, the emission lines

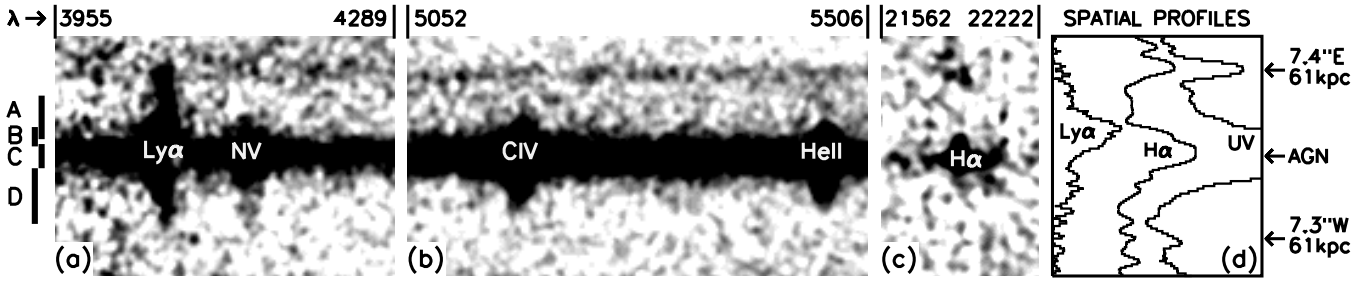

Figure 2. Distribution of line and continuum emission along the slit. Panels(a)–(c) show cutouts from the two-dimensional spectra, smoothed by an FWHM = 0.″7 Gaussian. The spatial axis (vertical) is centered on the UV continuum peak (AGN); the dispersion axis (horizontal) is discontinuous, with wavelength ranges (Å) given above the panels. Major emission lines are labeled in white. Panel (d) shows spatial profiles of continuum-subtracted Lyα and Hα emission, and the rest-frame UV continuum between C IV and He II. The apparent Lyα distribution differs very slightly between (a) and (d) due to continuum subtraction in the latter.

Table 1
Lyα Polarization of TXS 0211−122

Ap.	Position (″)	λ-range (Å)	P (%)	P.A. (°)	Lyα/He II[a]	Comments
A	1.50–5.35 E	4046–4081	16.4 ± 4.6	154 ± 8	5.5 ± 0.8	East Lyα region
A	1.50–5.35 E	4067–4074	⩽6.8 (3σ)	···	5.5 ± 0.8	East Lyα region; line core only
A	1.50–5.35 E	4046–4081	23.1 ± 7.1	143 ± 8	5.5 ± 0.8	East Lyα region; continuum-subtracted
B	0.86–2.57 E	4046–4081	<10.6 (3σ)	···	2.0 ± 0.2	At the spatial peak of Lyα
C	1.07 W–1.07 E	4046–4077	<4.7 (3σ)	···	0.42 ± 0.02	At the spatial peak of UV continuum
D	1.07–5.99 W	4053–4081	<27.6 (3σ)	···	1.3 ± 0.2	Western Lyα nebula

Note. [a] Line ratio Lyα/He II λ1640, determined from the total line fluxes at the given spatial positions along the slit.

Table 2
Lyα Polarization in Aperture A for Different Combinations of the Four Integration Sets

Run	P (%)	P.A. (°)
1+2	16.6 ± 6.3	182 ± 10
1+3	25.4 ± 7.6	167 ± 8
1+4	10.2 ± 6.8	161 ± 18
2+3	26.2 ± 9.4	147 ± 8
2+4	14.3 ± 7.3	126 ± 14
3+4	35.7 ± 10.0	137 ± 6
1+2+3	19.2 ± 5.4	166 ± 8
1+2+4	9.1 ± 5.2	161 ± 17
1+3+4	19.9 ± 5.7	154 ± 8
2+3+4	23.9 ± 6.4	139 ± 7
1+2+3+4	16.4 ± 4.6	154 ± 8

C IV and He II have $P \leqslant 10\%$ and $P \leqslant 13\%$, respectively. The high surface brightness Lyα emission closer to the nucleus is also not significantly polarized (Apertures B and C: ⩽10.6% and ⩽4.7%), while in the western nebula the data do not provide the necessary sensitivity for useful constraints (Aperture D: $P \leqslant 27.6\%$).

As a check for our Lyα polarization detection in Aperture A, Table 2 lists Lyα polarization measurements using different combinations of the four runs. Although noisier, these measurements show generally good consistency.

This is the first detection of polarized narrow Lyα emission from a nebula associated with a radio-loud active galaxy, and only the second from an extragalactic nebula of any kind (Hayes et al. 2011; see also Prescott et al. 2011). Our measurement of $P = 16.4\% \pm 4.6\%$ for Lyα is consistent with the range in polarization predicted by models of Lyα scattering in H I halos around high-z galaxies (up to ∼40%; Dijkstra & Loeb 2008; Dijkstra & Kramer 2012). Together with the recent detection of polarized narrow Lyα in a high-z Lyα blob by Hayes et al. (2011), our new detection in TXS 0211−122 then suggests it may not be uncommon for Lyα nebulae at high redshift to be powered (at least partly) by scattering of Lyα by H I. Polarization measurements of a larger sample are now needed to ascertain whether or not this is generally the case for high-z Lyα nebulae.

As a minor detail, we note that the polarization P.A. (154° ± 8°) differs from that of the UV continuum by ∼30° (Table 3; also V01), implying that the resonantly scattered Lyα photons and dust-scattered UV continuum photons have different scattering geometries.

4. A 120 kpc GASEOUS SHELL AROUND THE Lyα NEBULA?

At the eastern edge of the Lyα nebula we detect a faint, unresolved continuum source (FWHM = 1.″1 ± 0.″1), positioned 7.″4 ± 0.″2 E (61 ± 2 kpc) along the slit, and a fainter one diametrically opposed at a position 7.″3 ± 0.″3 W (61 ± 2 kpc, Figure 2). The eastern source is polarized, with $P = 22\% \pm 6\%$ and P.A. = 182° ± 7° measured in the line-free region redward of the wavelength of the N V emission line, at 4260–4600 Å (or 1280–1380 Å in the rest frame). This polarization P.A. is close to perpendicular to the slit and to the radio source. For comparison, we measure $P = 21\% \pm 2\%$ and P.A. = 185° ± 2° in the same wavelength range using a 4.″1 aperture centered on the position of the central radio galaxy (see also V01). Like the radio galaxy, the eastern source shows a strong gradient (or decrement) in P toward longer wavelengths, falling to $P \leqslant 10\%$ in the continuum region between the expected wavelengths of C IV and He II. This wavelength dependence is consistent with a mixture of nebular continuum, which drops off sharply at $\lambda \lesssim 1300$ Å, and scattered light (V01).

Table 3
Properties of the Eastern Continuum Source and TXS 0211−122

Property	λ-interval	Eastern Source	TXS 0211−122[a]
Offset	4000–7000	$7\farcs4 \pm 0\farcs2$ E	$0\farcs0$
F_λ	4200–4300	5.1 ± 0.4[b]	23.0 ± 0.7[b]
F_λ	5250–5400	2.5 ± 0.2[b]	24.7 ± 0.3[b]
F_λ	6100–6290	3.3 ± 0.2[b]	20.1 ± 0.2[b]
Pol UV[c]	4260–4600	$22\% \pm 6\%$ $182^\circ \pm 7^\circ$	$21\% \pm 2\%$ $185^\circ \pm 2^\circ$
Pol UV[c]	5240–5430	$\leqslant 10\%$	$18\% \pm 1\%$ $188^\circ \pm 2^\circ$
F	Lyα	1.4 ± 0.2[d]	9.0 ± 0.3[d]
F	C IV	$\leqslant 0.4$[d]	28 ± 1[d]
F	He II	$\leqslant 0.3$[d]	15.7 ± 0.3[d]
F	Hα	7 ± 2[d]	64 ± 5[d]
F	[O III] 5007	$\leqslant 8$[d]	209 ± 4[d]
F	[O II] 3727	$\leqslant 11$[d]	25 ± 5[d]
Flux ratio	Lyα/He II	$\geqslant 4.7$	0.57 ± 0.01
Flux ratio	Lyα/Hα	0.20 ± 0.06	0.14 ± 0.02
Flux ratio	He II/Hα	$\leqslant 0.04$	0.25 ± 0.02
Flux ratio	[O III]/Hα	$\leqslant 1.1$	3.27 ± 0.02

Notes.
[a] Measured in an aperture of diameter $4\farcs1$, as also used by Vernet et al. (2001) and Humphrey et al. (2008b).
[b] 10^{-19} erg s^{-1} cm^{-2} Å^{-1}.
[c] Polarization (%) and P.A. (°) of the UV continuum.
[d] 10^{-17} erg s^{-1} cm^{-2}.

The eastern source is also detected in Hα (Figure 2), with FWHM $= 1000 \pm 300$ km s^{-1}, and $z = 2.335 \pm 0.004$ confirming its association with the radio galaxy. Such a high FWHM suggests turbulent, rather than gravitational, motion. Table 3 provides properties of this source, alongside those of the radio galaxy.

Previous modeling of the rest-frame ultraviolet emission from the extended narrow-line region of the radio galaxy has shown that it is powered predominantly by illumination by the central AGN (V01; Humphrey et al. 2008b). Interestingly, the spectral properties of the eastern source are very similar to those of the radio galaxy, in terms of the percentage and wavelength dependence of polarization, and also the relative fluxes of Lyα, Hα, and the UV continuum (Table 3). This, together with the fact that the polarization P.A. is perpendicular to the slit (and to the radio source), leads us to conclude that the eastern source is also powered by illumination by the AGN.

The western UV source is detected across the full wavelength range between Lyα and C III] λ1908, outside of which the sensitivity of the spectrum rapidly declines. Its continuum flux density is $0.6 \pm 0.2 \times 10^{-19}$ erg s^{-1} cm^{-2} Å^{-1} at 5300 Å. Unfortunately, we cannot ascertain its redshift because we detect no lines therefrom.

A natural explanation for the diametric opposition of the two UV sources is that they are the limb of a giant shell of gas and dust centered on the radio galaxy, detected in emission thanks to illumination by the active nucleus. Provided it has a sufficiently high covering factor, a shell like this also ought to be detected via strong, spatially extended absorption lines, including Lyα. Indeed, TXS 0211−122 does show a strong, spatially extended Lyα absorption feature in its spectrum when observed at moderate spectral resolution (van Ojik et al. 1997), as do around half of all radio-loud galaxies at high redshift (e.g., van Ojik et al. 1997; Binette et al. 2000; Baker et al. 2002; Humphrey et al. 2008a). These giant H I absorbers are usually interpreted in terms of a giant shell of gas enveloping the galaxy and its Lyα nebula (Binette et al. 2000). More specifically, TXS 0211−122 shows an H I absorber with a blueshift of $\sim$60 km s^{-1} from the Lyα emission, an observed diameter of $\geqslant 10''$ ($\geqslant$83 kpc) in the plane of the sky (comparable to the size of the Lyα-emitting nebula), a hydrogen column density of $N_{\rm H} \gtrsim 10^{18}$ cm^{-2}, and covering factor approaching unity (van Ojik et al. 1997).

We suggest that the diametrically opposed UV sources and the H I absorption are manifestations of a single structure: a shell of gas and dust enveloping the TXS 0211−122 and its Lyα nebula. If this shell has a radius of 61 kpc and a hydrogen column density of $N_{\rm H} \gtrsim 10^{18}$ cm^{-2}, its total gas mass would then be $\gtrsim 4 \times 10^8\ M_\odot$.

Although a pair of companion galaxies could be a potential alternative interpretation of the diametrically opposed UV sources, such a scenario would require a very fortuitous alignment between the two UV galaxies and TXS 0211−122. Deep narrowband imaging or integral field spectroscopy would allow a more definitive resolution of this issue.

5. DISCUSSION: THE ORIGIN OF THE Lyα NEBULA AND SHELL

We now propose a scenario for the origin of the Lyα nebula and the gaseous shell associated with TXS 0211−122. The presence of dust and metals in the shell argue strongly for an internal origin for this structure rather than an external one (e.g., infall). We suggest that this shell is the result of a starburst event in the central galaxy, during which mechanical energy was deposited into the interstellar medium by supernova explosions, to produce expanding bubbles of gas. The bubbles produced by the individual supernovae sweep up material from the interstellar medium, merging with other bubbles as they expand, to eventually form a single superbubble of gas and dust centered on the galaxy. In the presence of a sufficiently luminous background source (e.g., the central radio galaxy), this bubble will manifest itself as a spatially extended, narrow Lyα absorption feature with a blueshift with respect to the velocity of the Lyα *emission* (e.g., Tenorio-Tagle et al. 1999; Binette et al. 2000). Moreover, depending on its properties, such as

covering factor, radius, column density, etc., the shell may also be detectable in emission where it intersects the radiation beams of the active nucleus (Humphrey et al. 2013), as appears to be the case in TXS 0211−122.

In its wake, the superbubble can be expected to leave behind condensations of infalling gas, resulting from energy dissipation during collisions between individual bubbles, or from blowouts due to mass-loading. When irradiated by the AGN, these condensations will emit narrow emission lines and thus may appear as an extended, infalling, ionized nebula around the galaxy (e.g., Humphrey et al. 2007; Villar-Martín et al. 2007; Adams et al. 2009).

How many supernovae would be required to power the expansion of the shell? Assuming an expansion velocity of $\sim$60 km s^{-1} and gas mass of $\geqslant 4 \times 10^8\ M_\odot$ (see Section 4), then the kinetic energy of the shell would be $\gtrsim 10^{55}$ erg. A single core-collapse supernova will release 10^{51} erg of kinetic energy, of which $\sim$10% can contribute to producing and powering the shell (e.g., Thornton et al. 1998). A total of $\gtrsim 10^5$ supernovae would then be required, in turn requiring the formation of $\gtrsim 10^7\ M_\odot$ of stars (e.g., Heckman et al. 1990). Although TXS 0211−122 shows no clear evidence for ongoing star formation (V01), *Spitzer* Infrared Array Camera photometry does permit a star formation rate of up to $\sim 200\ M_\odot$ yr^{-1}, while also constraining the stellar mass to be $\leqslant 1.4 \times 10^{11}\ M_\odot$ (G. Drouart et al., in preparation).

Although it has been suggested that powerful radio jets can also sweep interstellar gas into shells (e.g., Krause 2002), we believe this would not provide a natural explanation in the case of TXS 0211−122. Our main objection is that a spatial correlation between the radio hot spots and the limb of the shell, which would be expected if the shell is driven by the jets, is not observed. That is, the eastern radio source has an observed length of $\sim$50 kpc, and the western one has a length of $\sim$90 kpc (Carilli et al. 1997), both of which are very different to the 61 kpc radius of the shell.

6. CONCLUSIONS

We have analyzed deep spectropolarimetry and spectroscopy of the $z = 2.34$ radio galaxy TXS 0211−122 and its gaseous environment, aiming to understand the origin, geometry, and power source of high-redshift Lyα nebulae.

Although the polarization of Lyα is low centrally ($P < 4.7\%$), it rises to $P = 16.4\% \pm 4.6\%$ at a distance of $\geqslant$12 kpc (1.″5) east of the galactic nucleus. This indicates that the giant Lyα nebula is partly powered by the scattering of centrally produced Lyα photons in a spatially extended gaseous envelope. This is the first detection of polarized Lyα emission to date from a nebula around a radio-loud active galaxy, and only the second from any extragalactic Lyα nebula.

At the extreme edges of the Lyα nebula, at a radius corresponding to 61 kpc, we have detected a pair of diametrically opposed UV sources. We have suggested that they are the limb of a dusty, gaseous shell surrounding the Lyα nebula, seen in illumination, thanks to the presence of the powerful active nucleus in TXS 0211−122.

We have argued that the observed configuration of the gaseous environment of TXS 0211−122 can be naturally understood in terms of the expansion of a starburst-driven bubble through the galaxy and its gaseous halo, spreading metals and dust out to radii of $\sim$61 kpc.

A.H. acknowledges a Marie Curie Fellowship cofunded by the 7th Research Framework Programme and the Portuguese Fundação para a Ciência e a Tecnologia. Some of the data presented herein were obtained at the W. M. Keck Observatory, which is operated as a scientific partnership among the California Institute of Technology, the University of California and the National Aeronautics and Space Administration. The Observatory was made possible by the generous financial support of the W. M. Keck Foundation. We also thank the referee for useful comments.

REFERENCES

Adams, J. J., Hill, G. J., & MacQueen, P. J. 2009, ApJ, 694, 314
Baker, J. C., Hunstead, R. W., Athreya, R. M., et al. 2002, ApJ, 568, 592
Binette, L., Kurk, J. D., Villar-Martín, M., & Röttgering, H. J. A. 2000, A&A, 356, 23
Binette, L., Wilman, R. J., Villar-Martín, M., et al. 2006, A&A, 459, 31
Carilli, C. L., Roettgering, H. J. A., van Ojik, R., Miley, G. K., & van Breugel, W. J. M. 1997, ApJS, 109, 1
Dijkstra, M., & Kramer, R. 2012, MNRAS, 424, 1672
Dijkstra, M., & Loeb, A. 2008, MNRAS, 386, 492
Fosbury, R. A. E., Villar-Martín, M., Humphrey, A., et al. 2003, ApJ, 596, 797
Goodrich, R. W., Cohen, M. H., & Putney, A. 1995, PASP, 107, 179
Haiman, Z., Spaans, M., & Quataert, E. 2000, ApJL, 537, L5
Hayes, M., Scarlata, C., & Siana, B. 2011, Natur, 476, 304
Heckman, T. M., Armus, L., & Miley, G. K. 1990, ApJS, 74, 833
Humphrey, A., Binette, L., Villar-Martín, M., Aretxaga, I., & Papaderos, P. 2013, MNRAS, 428, 563
Humphrey, A., Villar-Martín, M., Fosbury, R., Vernet, J., & di Serego Alighieri, S. 2006, MNRAS, 369, 1103
Humphrey, A., Villar-Martín, M., Fosbury, R., et al. 2007, MNRAS, 375, 705
Humphrey, A., Villar-Martín, M., Sánchez, S. F., et al. 2008a, MNRAS, 390, 1505
Humphrey, A., Villar-Martín, M., Vernet, J., et al. 2008b, MNRAS, 383, 11
Krause, M. 2002, A&A, 386, L1
Moorwood, A., Cuby, J.-G., Biereichel, P., et al. 1998, Msngr, 94, 7
Mori, M., & Umemura, M. 2006, Natur, 440, 644
Oke, J. B., Cohen, J. G., Carr, M., et al. 1995, PASP, 107, 375
Prescott, M. K. M., Dey, A., Brodwin, M., et al. 2012, ApJ, 752, 86
Prescott, M. K. M., Dey, A., & Jannuzi, B. T. 2009, ApJ, 702, 554
Prescott, M. K. M., Smith, P. S., Schmidt, G. D., & Dey, A. 2011, ApJL, 730, L25
Simmons, J. F. L., & Stewart, B. G. 1985, A&A, 142, 100
Smith, D. J. B., & Jarvis, M. J. 2007, MNRAS, 378, L49
Steidel, C. C., Adelberger, K. L., Shapley, A. E., et al. 2000, ApJ, 532, 170
Taniguchi, Y., & Shioya, Y. 2000, ApJL, 532, L13
Tenorio-Tagle, G., Silich, S. A., Kunth, D., Terlevich, E., & Terlevich, R. 1999, MNRAS, 309, 332
Thornton, K., Gaudlitz, M., Janka, H.-T., & Steinmetz, M. 1998, ApJ, 500, 95
van Ojik, R., Roettgering, H. J. A., Miley, G. K., & Hunstead, R. W. 1997, A&A, 317, 358
van Ojik, R., Rottgering, H. J. A., Miley, G. K., et al. 1994, A&A, 289, 54
Vernet, J. 2000, PhD thesis, Univ. Paris VII
Vernet, J., Fosbury, R. A. E., Villar-Martín, M., et al. 2001, A&A, 366, 7 (V01)
Villar-Martín, M., Binette, L., & Fosbury, R. A. E. 1996, A&A, 312, 751
Villar-Martín, M., Sánchez, S. F., Humphrey, A., et al. 2007, MNRAS, 378, 416
Villar-Martín, M., Vernet, J., di Serego Alighieri, S., et al. 2003, MNRAS, 346, 273
Wilman, R. J., Gerssen, J., Bower, R. G., et al. 2005, Natur, 436, 227
Zheng, Z., Cen, R., Weinberg, D., Trac, H., & Miralda-Escudé, J. 2011, ApJ, 739, 62